

Best-first search guided multistage mass spectrometry-based glycan identification
—Supplementary Materials—

January 16, 2019

Contents

List of Tables

List of Figures

Table S. 1: Standard glycan samples

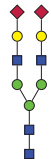
<i>Man-5D1</i>	<i>Man-6</i>	<i>Man-7D3</i>	<i>Bi-AntiA2</i>	<i>Hybrid-Octa</i>	<i>NGA3</i>	<i>NGA4</i>
						

Table S. 2: Comparison of performance of bestFSA with depth-first-search (DFS) and breadth-first-search (BFS) on seven glycan standards.

Name	Num of candidates	BFS		DFS		bestFSA	
		Prob.	Rds	Prob.	Rds	Prob.	Rds
<i>Man-5D1</i>	12	0.75	4	0.75	10	0.75	2
<i>Man-6</i>	12	0.10	6	0.89	9	0.75	3
<i>Man-7D3</i>	9	0.93	5	0.73	14	0.93	3
<i>Bi-AntiA2</i>	2	0.90	1	0.90	1	0.90	1
<i>Hybrid-Octa</i>	9	0.10	2	0.10	2	0.82	2
<i>NGA3</i>	7	0.89	2	0.89	2	0.92	2
<i>NGA4</i>	5	0.95	3	0.72	4	0.73	2

The bestFSA successfully identified all seven glycan standards within a maximum of 3 rounds of MSⁿ experiments (MS¹ did not count). DFS and BFS generally required more rounds of MSⁿ than bestFSA.

Table S. 3: Reproducibility of the entire identification process including the acquisition of MSⁿ spectra guided by the bestFSA.

Glycan	MNa ⁺	Num of candidates	standard			
			MS ¹	MS ²	MS ³	MS ⁴
<i>Man-5D1</i>	1579	12	TEST1	0.48	<u>0.75</u>	
			TEST2	0.38	<u>0.70</u>	
<i>Man-6</i>	1783	12	TEST1	0.33	0.66	<u>0.75</u>
			TEST2	0.22	0.66	<u>0.87</u>
<i>Man-7D3</i>	1987	9	TEST1	0.32	0.57	<u>0.93</u>
			TEST2	0.29	0.52	<u>0.88</u>
<i>Bi-AntiA2</i>	2792	2	TEST1	0.90		
			TEST2	0.73		
<i>Hybrid-Octa</i>	1824	9	TEST1	0.42	<u>0.82</u>	
			TEST2	0.28	<u>0.71</u>	
<i>NGA3</i>	1906	7	TEST1	0.32	<u>0.92</u>	
			TEST2	0.31	<u>0.83</u>	
<i>NGA4</i>	2152	5	TEST1	0.23	<u>0.73</u>	
			TEST2	0.23	<u>0.74</u>	

BestFSA successfully identified all glycan standards in two independent tests with nearly identical performance. Candidate's probability exceeding the predefined threshold (0.70) were considered as identified and shown in underlined bold.

Table S. 4: Calculation of probabilities using different mass tolerance.

Glycan	MNa ⁺	Probability Using Different Mass Tolerance				
		0.1	0.5	0.6	1.0	2.0
<i>Man-5D1</i>	1579	0.54	0.75	0.72	0.70	0.26
<i>Man-6</i>	1783	0.75	0.75	0.75	0.72	0.72
<i>Man-7D3</i>	1987	0.82	0.93	0.93	0.93	0.80
<i>Bi-antiA2</i>	2792	0.90	0.90	0.90	0.90	0.65
<i>Hybrid-Octa</i>	1824	0.85	0.82	0.82	0.74	0.56
<i>NGA3</i>	1906	0.82	0.92	0.92	0.92	0.82
<i>NGA4</i>	2152	0.58	0.73	0.73	0.68	0.73

For the present work, a mass tolerance was set at 0.5 although a value between 0.5-1.0 does not affect the results

Table S. 5: Effect of collision energy on the results of bestFSA .

MS2 CID energy (mV)	Precursor-ion remained (%)	MS ² probability	Selected peak for MS ³	Probability after MS ³
110	100	0.30	1084	0.86
120	100	0.30	1084	0.82
130	50	0.39	1084	0.85
200	10	0.39	1084	0.87
300	0	0.39	1084	0.85

¹ We have now provided these data using Man-6 as the example.

² Different collision energy may produce product-ion spectra with different appearance. In extremely cases if the energy is too low the molecule can fragment while if the energy is too high the molecule can break into small pieces by non-specific fragmentation resulting in no structural information. These two extreme cases can be readily avoided. As the collision energy is broadly related to the size of glycans, based on our experience, we set the collision energy at 100-400 mV. Within the normally used energy rang, although the intensities of fragment ions may be different, the results remain roughly the same.

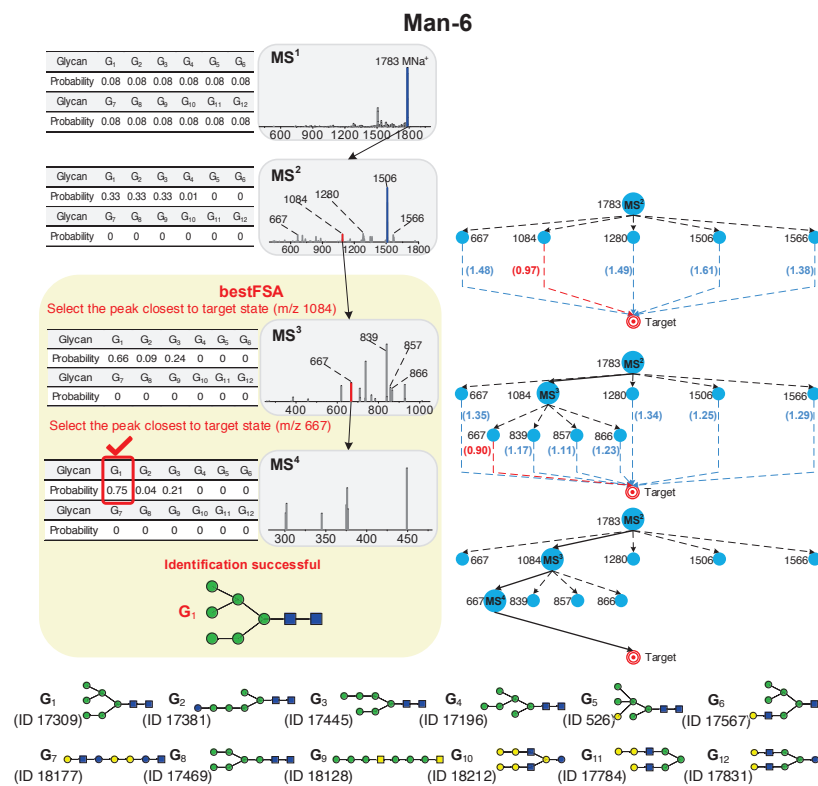


Figure S. 1: **Identification process of *Man6* using bestFSA.** Four rounds of mass spectrometric scanning (MS¹, MS², MS³, MS⁴) were required to assign *Man6* from the 12 candidate glycans G₁ to G₁₂ (structures together with CarbBank ID numbers listed in the box at the bottom). Middle column: mass spectrometry process; left column: calculated probabilities; and right column: distance calculation process. The fragment ion shown in red was selected as the precursor for the next round of product-ion scanning. The calculated distances are in brackets along the virtual path to the target state.

Man-5D1

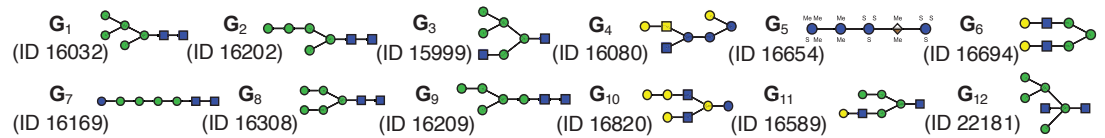
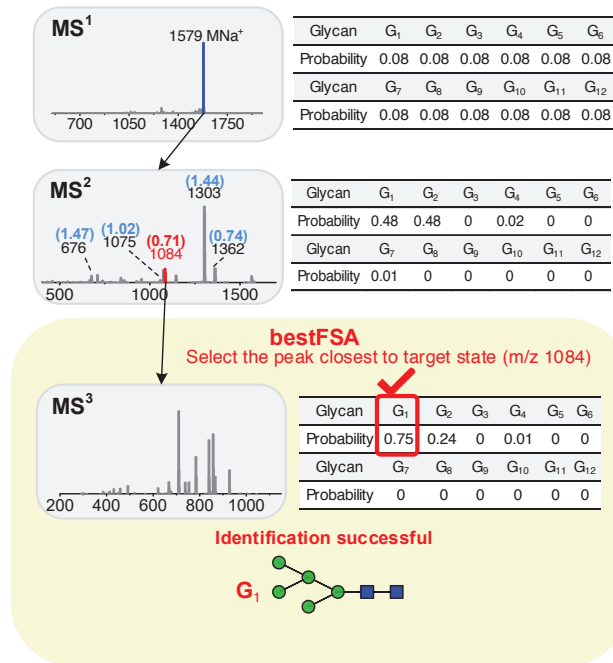


Figure S. 2: Identification process of *Man-5D1* using bestFSA.

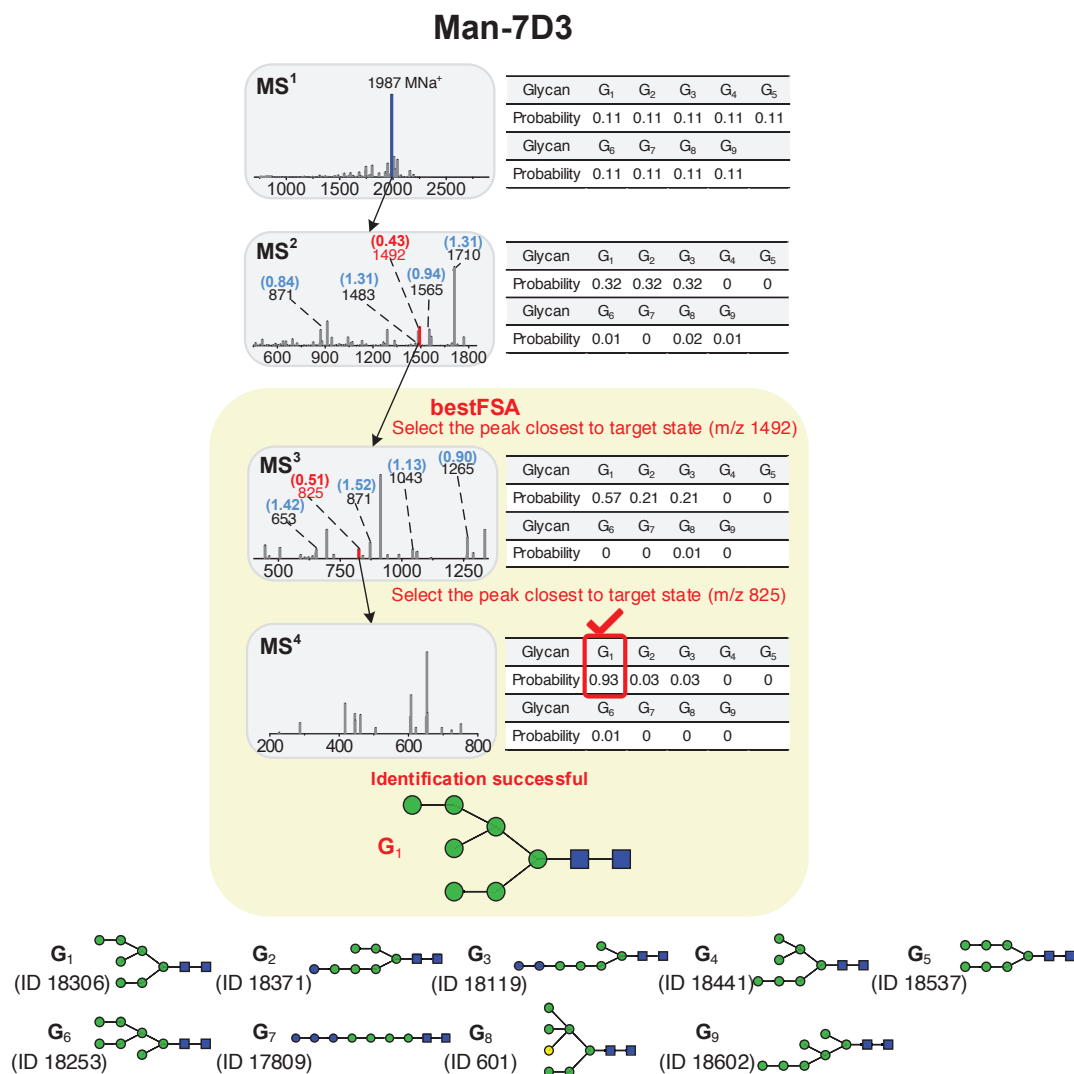


Figure S. 3: Identification process of *Man-7D3* using bestFSA.

Bi-AntiA2

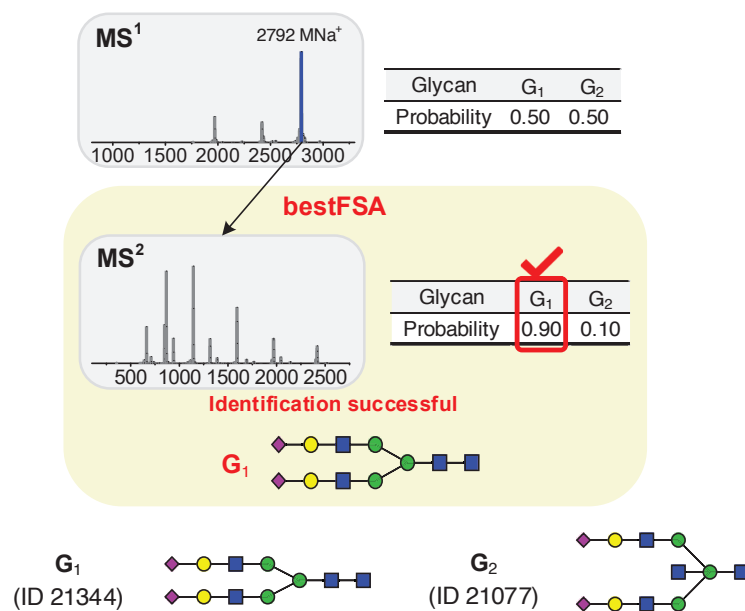


Figure S. 4: Identification process of *Bi-AntiA2* using bestFSA.

Hybrid-Octa

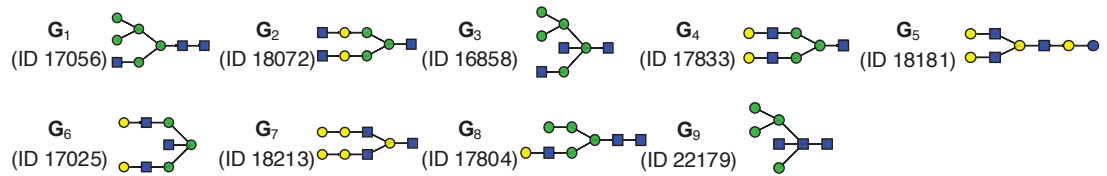
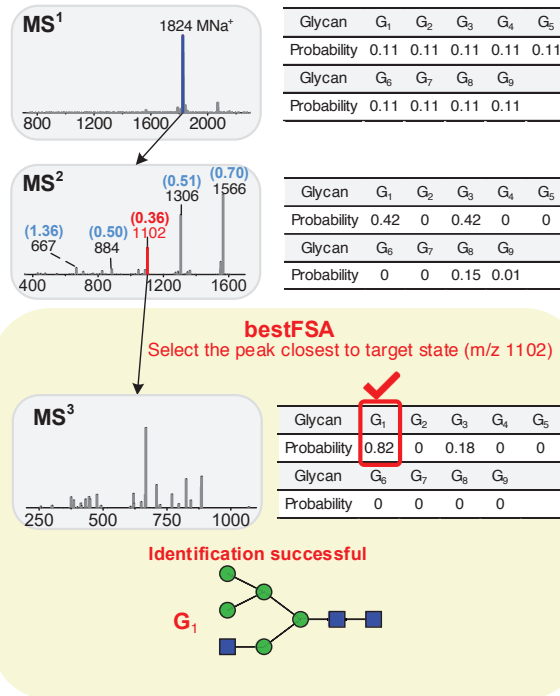


Figure S. 5: Identification process of *Hybrid-Octa* using bestFSA.

NGA3

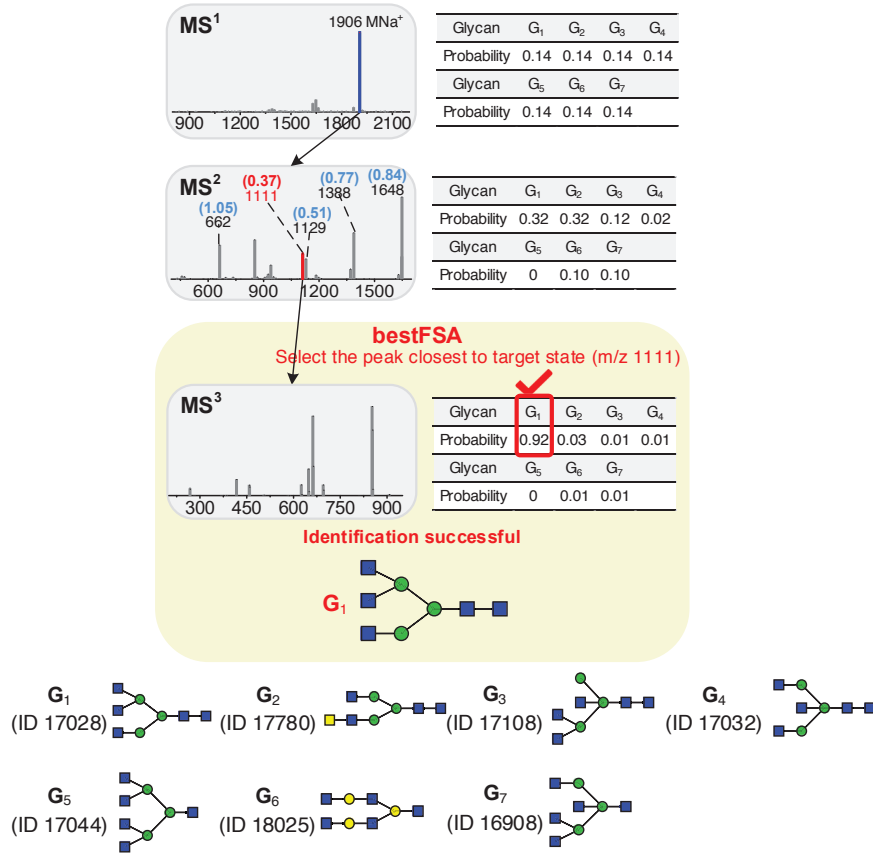


Figure S. 6: Identification process of *NGA3* using bestFSA.

NGA4

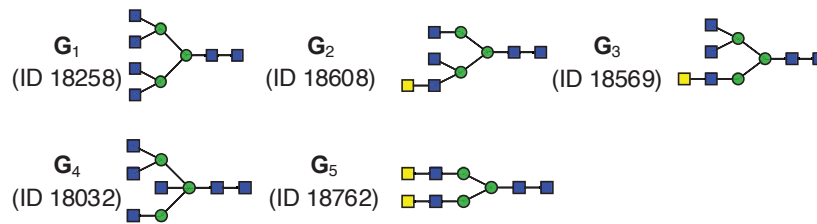
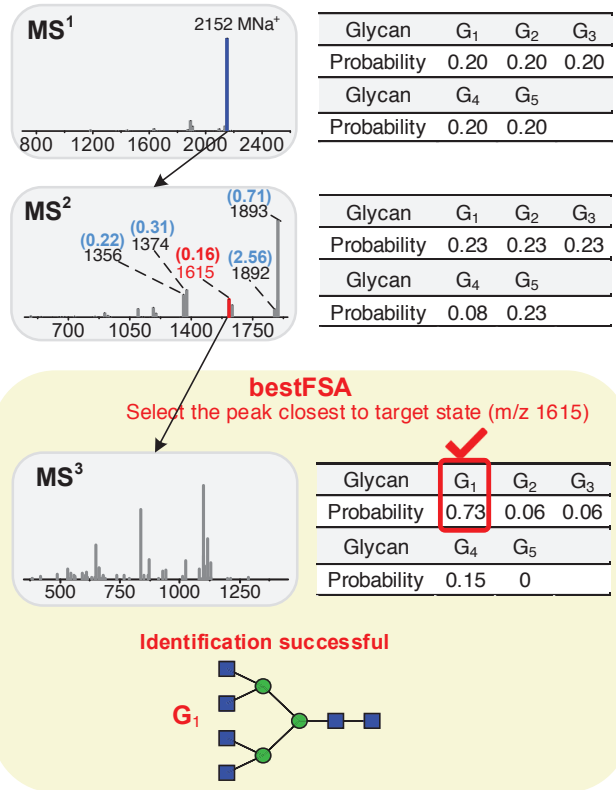


Figure S. 7: Identification process of *NGA4* using bestFSA.

Man9

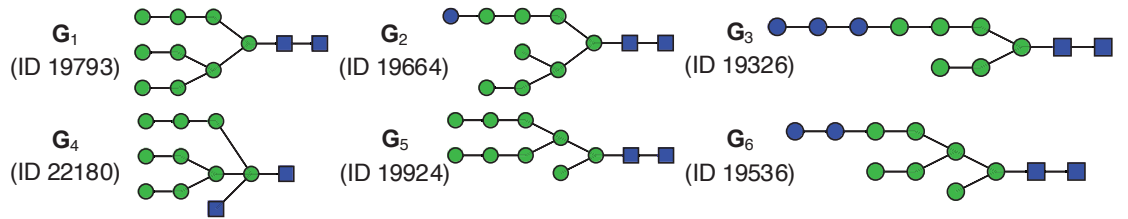
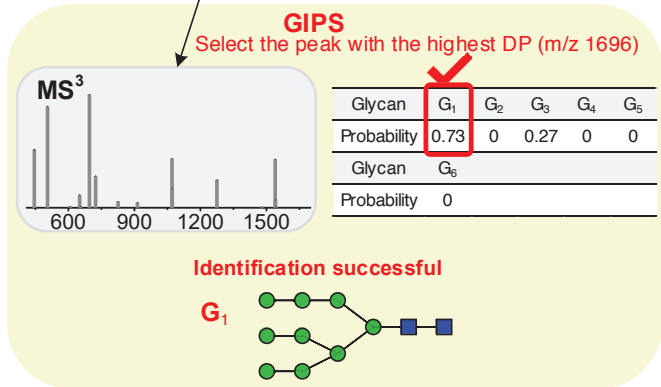
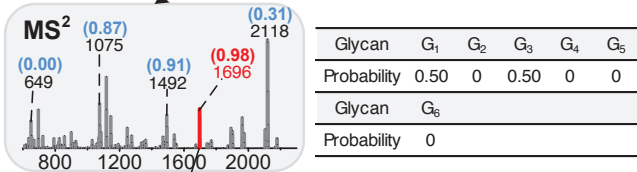
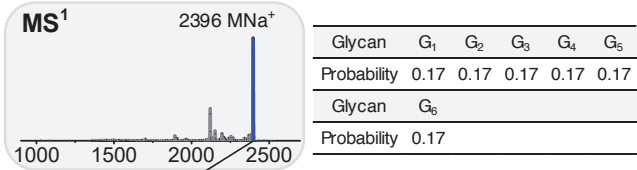


Figure S. 8: Identification process of *Man9* using bestFSA.